

Article

Simulated Annealing Algorithm for Wind Farm Layout Optimization: A Benchmark Study

Kyoungboo Yang¹ and Kyungho Cho^{2,*}

¹ Faculty of Wind Energy Engineering, Jeju National University, 102 Jejudaehakno, Jeju 63243, Korea; kbyang@jejunu.ac.kr

² Department of Mechatronics Engineering, Jeju National University, 102 Jejudaehakno, Jeju 63243, Korea

* Correspondence: khcho@jejunu.ac.kr; Tel.: +82-64-754-3711

Received: 15 October 2019; Accepted: 18 November 2019; Published: 20 November 2019



Abstract: The optimal layout of wind turbines is an important factor in the wind farm design process, and various attempts have been made to derive optimal deployment results. For this purpose, many approaches to optimize the layout of turbines using various optimization algorithms have been developed and applied across various studies. Among these methods, the most widely used optimization approach is the genetic algorithm, but the genetic algorithm handles many independent variables and requires a large amount of computation time. A simulated annealing algorithm is also a representative optimization algorithm, and the simulation process is similar to the wind turbine layout process. However, despite its usefulness, it has not been widely applied to the wind farm layout optimization problem. In this study, a wind farm layout optimization method was developed based on simulated annealing, and the performance of the algorithm was evaluated by comparing it to those of previous studies under three wind scenarios; likewise, the applicability was examined. A regular layout and optimal number of wind turbines, never before observed in previous studies, were obtained and they demonstrated the best fitness values for all the three considered scenarios. The results indicate that the simulated annealing (SA) algorithm can be successfully applied to the wind farm layout optimization problem.

Keywords: wind energy; wake effect; wind farm layout optimization; heuristic optimization; simulated annealing algorithm

1. Introduction

One of the key aspects of wind farm design is to determine the position of the wind turbines within a given area, and one of the main objectives of this wind turbines layout is to minimize the wake effect between wind turbines. The wake generated by upstream wind turbines causes wind speed reduction resulting in power losses in the downstream wind turbines. In addition, the unstable turbulent flow caused by the wake increases the fatigue load of those wind turbines affected by the wake. The wind speed deficit by the wake effect can be estimated using a wake model. However, it is difficult to optimize the wind turbine layout by considering the range of effects of the wake that changes according to the wind direction. To solve the complex wind farm layout optimization (WFLO) problem, various layout optimization methods have been introduced, and many related studies addressed this [1,2]. The first study was published in 1994 by Mosetti et al. [3], where they introduced the genetic algorithm (GA), now considered one of the most typical optimization methods to address the WFLO problem. Although the wind farm model applied by Mosetti's study is not a practical model, their proposed model and the wind scenario have been used as a comparative benchmark to examine the performance of various algorithms.

In general, the optimization methodology for the WFLO problem can be divided into heuristic and mathematical programming methods. A heuristic is a method of searching for an optimal solution based on probabilistic theory, and mathematical programming is a method of formulating and optimizing the variables and boundary conditions of a problem. Algorithms that use heuristic methods for the WFLO problem include the GA [3–19], evolutionary strategy [20–22], particle swarm optimization [23–25], and greedy heuristic [26,27]. Moreover, other works on the development of various algorithms have been conducted [28–33]. Among these methods, GA is the most widely used. GA is a representative optimization algorithm of heuristic methodology based on the concept of the evolution of nature. Although it considers a cooperative system of the population, the optimal solution may vary depending on the number of populations and generations, and it is difficult to exactly determine these factors. However, GA is still actively used in various fields owing to its versatility. The mathematical programming method includes mixed-integer programming [34–37] and gradient-based optimization [38–41]. Unlike heuristics methods, it has the advantage of ensuring global optimization. However, it works appropriately only in the cases when a given problem can be expressed as a complete function mathematically. The WFLO problem falls into the class of problems called combinatorial optimization, and due to its computational complexity and discrete constraints, it is difficult to express it as a complete mathematical function to find an optimal solution [29]. Therefore, mathematical programming methods are not suitable for wind farm design because of the properties (non-linear, multi-modal, discontinuous) of the WFLO problem [1,2].

The optimization methodology for the WFLO problem developed in this study is a method using the simulated annealing (SA) algorithm. The SA algorithm simulates the annealing process in metallurgy which increases the rigidity of metal materials. Similar to the GA, the SA algorithm is one of the representative heuristic approaches that was developed based on the natural law [42]. Although the GA is the most widely used algorithm for the WFLO problem, SA is also one of the most popular methods among heuristic methodologies in the optimization field. In particular, in the SA algorithm, the process of simulating the annealing process of crystal structures inside the metal under temperature conditions is similar to the situation in which the turbines are placed at promising locations in the wind farm. Furthermore, unlike GA, in which various structures may exist depending on the design purpose, the SA algorithm structure is consistent. The SA algorithm is also a representative optimization algorithm, but despite its usefulness, it has not been widely applied to wind farm layout optimization. Therefore, in this study, we developed an SA algorithm for the wind farm layout optimization problem. Subsequently, we compared and evaluated the SA algorithm to those presented in previous studies.

To compare and evaluate the performance of an algorithm, a reference target in which the algorithm is applied is needed. Mosetti's study mentioned above has been used in numerous studies to evaluate the performance of various algorithms for wind farm layout optimization. Grady et al. [4] developed a GA with a subpopulation and compared the results to Mosetti's findings which yielded more efficient layout results than Mosetti's. They mentioned that although GA was an effective global optimization method, it was necessary for a sufficient number of populations and generations and that large computational costs could be incurred due to the large number of independent variables. González et al. [8] also used a GA and compared their results to Grady's study. They resulted in improved energy efficiency and shortened calculations compared to Grady. Zhang et al. [9] adopted the greedy algorithm and compared it to Mosetti and Grady, and derived enhanced layout results using more wind turbines than previous studies. Parada et al. [19] compared their results to Grady's study and demonstrated that there was an optimized layout of the regular pattern in the same wind farm model as previous studies. Most studies compared their results to Mosetti and Grady's studies to evaluate their developed algorithms. Mosetti's case studies are considered to be the basis for evaluating algorithms in the development of the wind farm layout optimization algorithm.

In this study, we propose a new methodology for wind farm layout optimization using the SA algorithm. Various optimization methodologies have been developed in the past, but the SA algorithm

has not been widely applied, despite its advantages. Therefore, this study aims to secure a variety of optimization methodologies for more efficient wind farm design. To evaluate the performance of the developed algorithm, a comparison was made under the same conditions as the previous studies, and the applicability of the developed algorithm was examined. In the actual wind farm design phase, various conditions (power cables, access road, prohibited area, geographical characteristics, etc.) must be reflected, but this study compared and evaluated the basic performance of the optimal placement algorithm, limited to wind farm efficiency and cost, which were the focusses of previous studies.

2. Methodology

2.1. Wake Model

One of the main goals of wind turbine layout is to minimize losses occurring due to wakes between turbines, and a wake model is necessary to calculate the wake losses. Many studies used the Jensen model [43], developed in 1983. Although the Jensen model was modified by Katic et al. in 1986 [44] and is now widely used in its updated form, in this study the initial Jensen model was used to compare the proposed algorithm considering the same conditions as in previous studies.

In the Jensen model, shown in Figure 1, it is assumed that the wake diameter increases linearly with an increase in distance and the wind speed distribution in the radial direction of the wake is identical. The wind speed deficit (δu) in the wake according to the distance x is as follows:

$$\delta u = u_0 \left(\frac{2a}{(1 + \alpha(x/r_1))^2} \right), \quad (1)$$

where u_0 is the free stream wind speed, a is the axial induction factor, and α is the entrainment constant. Wake expansion radius r_1 can be calculated as follows:

$$r_1 = r_0 \sqrt{\frac{1-a}{1-2a}}, \quad (2)$$

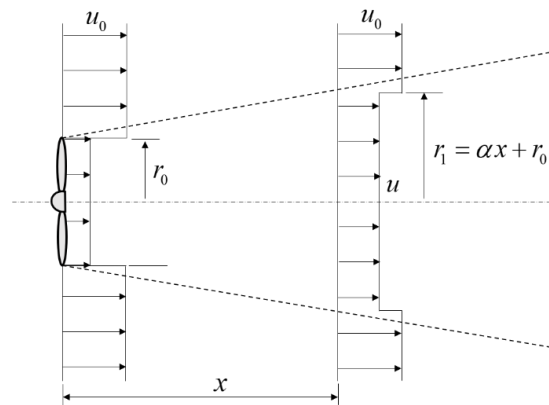


Figure 1. Schematic representation of the Jensen wake model.

The axial induction factor a can be calculated from the relationship with the thrust coefficient:

$$a = (1 - \sqrt{1 - C_t})/2, \quad (3)$$

The entrainment constant (also called the wake decay constant), which determines the size of the expanded wake behind the wind turbine, can be calculated with a surface roughness length (z_0) and hub height (h) of wind turbine by using the following formula:

$$\alpha = \frac{0.5}{\ln(h/z_0)}, \quad (4)$$

where z is the hub height of the wind turbine and z_0 is the surface roughness length of the wind farm.

The rotor of the wind turbine affected by the wake is fully or partially affected by single or multiple wakes depending on the wind direction, as shown in Figure 2. In the case of a wind turbine that is partially affected (Figure 2a), the wind speed deficit can be calculated as the ratio of the intersecting area between the wake and rotor to the rotor area:

$$\delta u = u_0 \left(\frac{2a}{(1 + \alpha(x/r_1))^2} \right) \frac{A_{overlap}}{A_r}, \quad (5)$$

where A_r is the rotor swept area of the wind turbine, and $A_{overlap}$ is the area of intersection of the wake and wind turbine rotor.

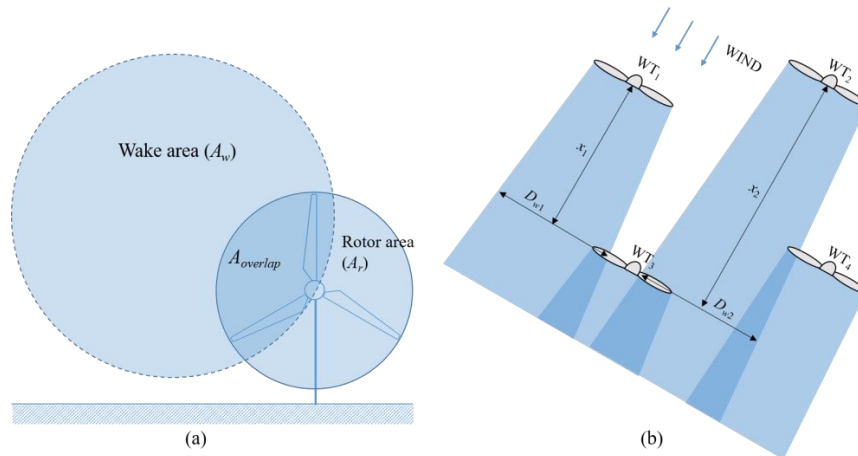


Figure 2. Partial and multiple wake effects: (a) Overlap area between the wake and rotor areas; (b) Multiple wake according to wind direction.

The wind speed deficit due to multiple wakes (Figure 2b), generated by N upstream wind turbines, can be calculated as follows:

$$\delta u_j = \sqrt{\sum_{i=1}^N \delta u_i^2}, \quad (6)$$

2.2. Cost Model and Objective Function

The key goal of the optimization algorithm is to minimize or maximize the given objective function. The objective function is defined according to the objective to be optimized as the target value for the optimization problem. Mosetti et al. proposed an objective function that takes into account the investment costs and total output of wind turbines to determine their optimal number and location within a given wind farm area. The investment cost of implementing wind turbines was modeled by considering only the total number of wind turbines (N) installed. Mosetti assumed that the nondimensionalized cost per year (cost/year) of a single wind turbine is one with a maximum

reduction in cost of 1/3 for each additional wind turbine. Therefore, the total cost (C_{total}) per year for a wind farm can be expressed as follows:

$$C_{total} = N \left(\frac{2}{3} + \frac{1}{3} e^{-0.00174N^2} \right), \quad (7)$$

The objective function (F) for optimization is defined as a function of the cost versus total output:

$$F = \frac{C_{total}}{P_{total}}, \quad (8)$$

where P_{total} is the total output obtained considering the wake effect in a wind farm, which can be calculated with values in Table 1, as follows:

$$P_{total} = \sum_{i=1}^N \frac{1}{2} \rho A u_i^3 C_p = \sum_{i=1}^N (0.5 \times 1.225 \times \pi \times 20^2 \times 0.39 \times 0.001) \approx \sum_{i=1}^N 0.3 u_i^3, \quad (9)$$

where ρ is the air density, A is the rotor swept area, and C_p is the power coefficient.

Table 1. Properties of Wind Turbines and Wind Farm.

Property	Value	Property	Value
Hub height (h)	60 m	Wind farm size	2 × 2 km
Rotor diameter (D)	40 m	Surface roughness length (z_0)	0.3 m
Thrust coefficient (C_t)	0.88	Air density (ρ)	1.225 kg/m ³
Power coefficient (C_p)	0.39	Spacing	200 m (5D)
Axial induction factor (a)	0.326	Entrainment constant (α)	0.094

Apart from the cost of wind farms, the park efficiency (E_p) related to examining the wind turbine layout efficiency can be calculated as follows:

$$E_p = \frac{P_{total}}{N(0.3u^3)}, \quad (10)$$

2.3. Wind Farm and Wind Scenarios

In the present study, the wind farm model used to perform the wind farm layout optimization is a hypothetical wind farm which was used by Mosetti. The wind farm has a square grid as the computational domain divided into 100 square cells, where a wind turbine is placed at the center. Figure 3 shows a grid of the wind farm, where each cell is equal to five rotor diameters (5D, 200 m × 200 m), the square grid has 10 columns and 10 rows of cells, and the total wind farm size is 2 km × 2 km. In the wind farm, wind turbines with a rotor diameter of 40 m are placed at the center of the cell, maintaining a 5D separation distance between the wind turbines. The specifications of the wind turbines and the wind farm that are applied to the layout optimization, which are the same as those in the previous studies, are presented in Table 1.

To evaluate the performance of the optimization algorithm, three wind speed scenarios were considered for the case studies, as follows: (a) the constant wind speed and single wind direction, (b) the constant wind speed and multiple wind direction, and (c) the variable wind speed and multiple wind direction. Case study (a) assumes that the wind speed of 12 m/s blows only from the north, and this can be used to confirm the basic performance of the wake model and the layout algorithm. Case study (b) is when the azimuth angle is divided into 36 sections, and the wind speed of 12 m/s is generated from all 36 wind directions with a uniform probability. Case study (c) considers 36 wind directions similar to that of case study (b) and includes three wind speeds (8, 12, and 17 m/s) with different probabilities of occurrence, as shown in Figure 4. We can see that the occurrence frequencies

of 12 m/s and 17 m/s wind speed between 270 and 350° of wind direction are greater as compared to those in other directions, which means NW is the prevailing wind direction of the wind farm. Thus, wind directions between 270 and 350° have a greater effect on the wind farm layout as compared to the other directions. This condition is quite different from the wind condition of the actual wind farm, but it is used for comparing and evaluating the performance of the optimal layout algorithm.

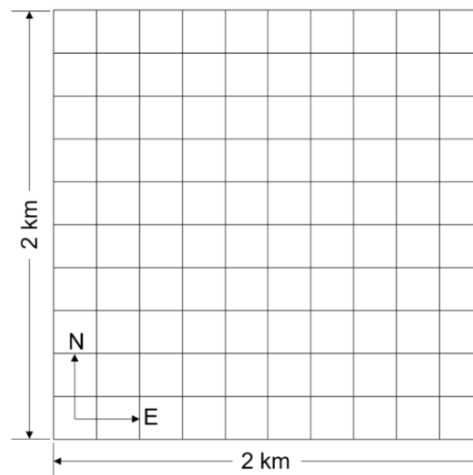


Figure 3. Wind farm grid for the layout optimization.

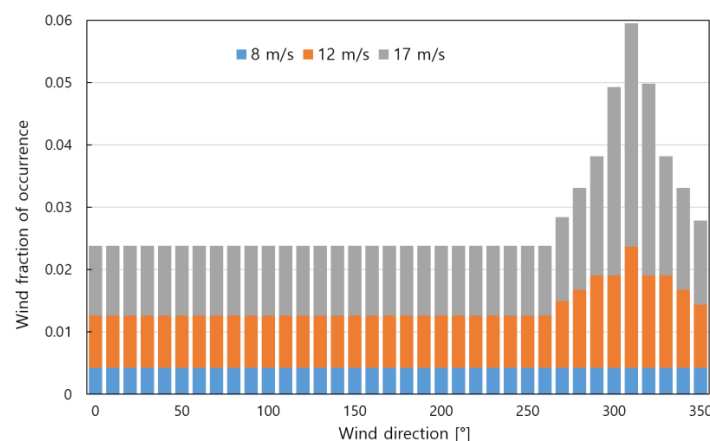


Figure 4. Wind fraction of the probability of occurrence by direction for case study (c).

2.4. Optimization Methodology

The SA algorithm is a method to simulate the metallurgical annealing process, in which the internal energy is minimized by changing the internal crystal structure of a metal, while the metal material is gradually cooled down [42]. In real metals, the repositioning of internal crystals increases the rigidity of the metal. From an algorithmic perspective, this process can be seen as finding an optimal solution in a global optimization problem. In the WFLO problem, this process can be used for determining the optimal layout result for the wind turbine by changing the position of the wind turbine. The temperature is one of the computational parameters of an SA algorithm for process iterations and probability calculations to search for the optimal solution. The optimal solution is searched for depending on the probability by varying this virtual temperature parameter [45].

Algorithm 1. Pseudocode of Simulated Annealing for the Wind Farm Layout Optimization.

Input: Problem size, Initial temperature (T), Stopping temperature (T_{\min})
Temperature control (α), Number of iteration (Markov number)

```

1:  $L_{\text{current}} = \text{create}(\text{Problem size})$  // Create and initialize layout of wind turbines
2:  $L_{\text{best}} = L_{\text{current}}$ 
3: while  $T > T_{\min}$  do
4:   for  $i = 1$  to Markov number do
5:      $L_i = \text{perturbation}(L_{\text{current}})$  // Perturbation of wind turbine position
6:      $\Delta \text{cost} = \text{cost}(L_i) - \text{cost}(L_{\text{current}})$  // Evaluation of cost
7:     if  $\Delta \text{cost} < 0$  then  $L_{\text{current}} = L_i$ 
8:     if  $\text{cost}(L_{\text{current}}) < \text{cost}(L_{\text{best}})$  then
9:        $L_{\text{best}} = L_{\text{current}}$ 
10:    end if
11:    else if  $\exp(-\Delta \text{cost}/T) > \text{random}$  then // Metropolis criterion
12:       $L_{\text{current}} = L_i$ 
13:    end if
14:  end for
15:   $T = \alpha T$  // Decreasing temperature
16: end while

```

Output: Best layout of wind turbines (L_{best})

Algorithm 1 is a pseudocode that shows the process of the SA algorithm in the WFLO problem. The main elements in this code are the temperature control, perturbation, and metropolis criterion. The temperature control is a process of slowly lowering the temperature from the initial high value to the lower one, a process called the cooling schedule. This process affects the efficiency of the algorithm. A fast linear temperature decrease is more likely to converge to a local solution, and an exponential slow decrease requires a significant amount of time to complete the operation. Perturbation is the process of repositioning some of the wind turbines to find better locations for producing more energy; therefore, in this process, perturbation strategy is required in order to improve the layout. Metropolis criterion is a selection process that determines whether to accept a candidate solution or not. By default, candidate solutions will be accepted during the perturbation if the fitness improves. However, even a candidate layout ($L_{\text{candidate}}$) that became worse during the perturbation, depending on the probability of the Metropolis criterion, can be accepted as the current layout (L_{current}). This avoids the possibility of convergence to the local solution by following only those solutions for which the fitness is improved [46]. Fitness refers to the adaptation of the optimization process, which indicates whether the value of a given objective function has improved in the desired direction. The fitness value is the same as the objective function value. The Metropolis criterion based on the Metropolis-Hasting algorithm is as follows:

$$P_{\text{metro}} = \exp\left(-\frac{\Delta \text{cost}}{T}\right), \quad (11)$$

$$L_{\text{current}} = \begin{cases} L_{\text{candidate}}, & \text{if } P_{\text{metro}} > P_{\text{rand}} \\ L_{\text{current}}, & \text{otherwise} \end{cases}, \quad (12)$$

where P_{metro} is a metropolis probability, P_{rand} is a probability obtained using the random number generator function, and T is the current temperature parameter.

Summarizing the performance of the SA algorithm, when the initial temperature is high, the probability to select a solution by Metropolis criterion increases, resulting in active turbine movement and finding a location that produces higher energy in a wider search range. The temperature then slowly decreases, reducing the movement of the wind turbines (in this state, the wind turbines are in a somewhat energy-enhanced position) and confirming the final placement position.

Table 2 summarizes the parameters related to the SA algorithm performance. The initial temperature was set to 1.0 and was gradually decreased by temperature control ($\alpha = 0.98$) to finish

the layout process, when it reached 0.001. For each temperature step, the Markov number of 200 was used to determine the number of iterations of perturbation. The setting of parameters applied to the algorithm can vary depending on the nature and difficulty of the considered problem and can be determined by empirical or preliminary performance test. The initial temperature is essentially at 1.0 and the stopping temperature is recommended to be sufficiently low; however, when the stopping temperature is too low, a considerable amount of calculation time may be required. Therefore, an appropriate value can be selected by confirming the variation of fitness through a preliminary execution of the algorithm. For example, if the fitness value advances quickly to the desired value, then the stopping temperature can be set high; otherwise, it should be set low. Alternatively, a method for stopping the execution when the desired target value is reached can also be used, and this can be done without setting a stopping temperature. The temperature control typically uses the values in the range 0.85–0.98. The Markov number determines the amount of perturbation that will be performed. Generally, it should be set to more than 100 times. If the solution search range is larger, then this value should be increased.

Table 2. Parameters of the Layout Optimization.

Parameter	Value	Parameter	Value
Number of cells	10×10	Initial temperature	1.0
Cell size	200×200 m	Stopping temperature	0.001
Markov number	200	Temperature control (α)	0.98

3. Case Studies and Discussion

To evaluate the performance of the proposed layout optimization method based on the SA algorithm, the layout of wind turbines was performed for the three cases mentioned above, and the results were compared to those previously reported in the literature. There are several works based on this layout condition and scenarios proposed by Mosetti. However, despite showing the same layout results, the calculated values were different and the result value obtained in the present study differs as well. This can be explained due to a methodological difference in the calculation process using a wake model. However, some studies have demonstrated unreliable differences in the results. Therefore, the results of the present study were compared to those of five related studies (Mosetti et al. [3], Grady et al. [4], González et al. [8], Zhang et al. [9], and Parada et al. [19]) that provided the results within a reasonable range.

3.1. Case Study (a): Constant Wind Speed and Single Wind Direction

The first case study assumes that a 12 m/s wind is only blowing from the north and can expect that the turbines are positioned based on the north direction. Figure 5 shows the layout results obtained for case study (a), and the calculated values for the layout results are summarized in Table 3. To perform the comparison to the results of the present study, the results of the previous works are recalculated in the same way according to the layout position defined in each study, and for referencing purposes, the original values provided in each previous study are shown in parentheses in Table 3. The study by Mosetti deployed 26 turbines, while the study by Gray and other studies deployed 30 turbines. The results of the present study are the same as those obtained in the study by Gray et al. [4], which showed the efficiency and fitness better than the results reported in the study by Mosetti. As most of the studies show similar results, the results of case study (a) seem to be in the optimal layout. Figure 6 shows the fitness variation during the operation process of the SA algorithm in case study (a). At the beginning of the operation, it can be seen that the movement of turbines becomes more active due to the high-temperature parameter, and then the temperature is gradually decreased to stabilize. This behavior clearly shows the characteristics of the SA algorithm performance and also shows that the SA algorithm can be successfully applied to the wind farm layout optimization problem.

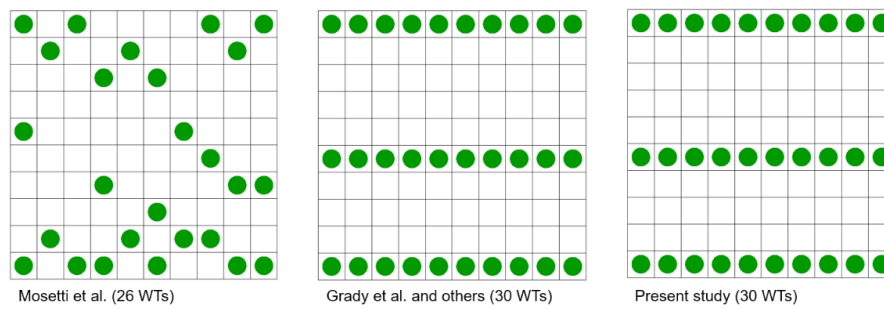


Figure 5. Layout results for case study (a).

Table 3. Layout Results for Case Study (a).

	Number of Turbines	Total Power (kW)	Efficiency (%)	Fitness Value
Mosetti et al. [3]	26	12,349 (12,352)	91.621 (91.645)	0.0016201 (0.0016197)
Grady et al. [4]	30	14,269 (14,310)	91.756 (92.015)	0.0015479 (0.0015436)
González et al. [8]	30	14,269 (not reported)	91.756 (–)	0.0015479 (–)
Parada et al. [19]	30	14,269 (14,785)	91.756 (95.068)	0.0015479 (0.0014940)
Zhang et al. [9]	30	14,269 (14,310)	91.756 (92.015)	0.0015479 (0.0015436)
Present study	30	14,269	91.756	0.0015479

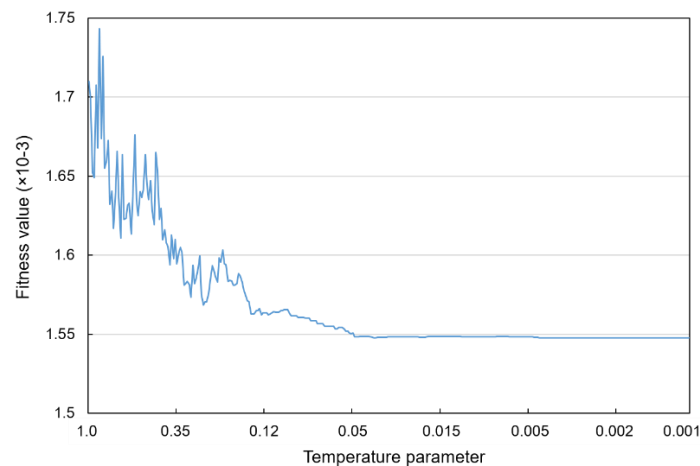


Figure 6. Fitness variation during the process in case study (a).

3.2. Case Study (b): Constant Wind Speed and Multiple Wind Directions

Case study (b) is the case where the 12 m/s wind speed is blown from 36 directions with a uniform probability, and the comparative results for this case are shown in Figure 7 and Table 4. Figure 7 shows different layout results, where it can be seen that the method proposed by Mosetti demonstrates the highest park efficiency; however, the fitness is the worst as 19 turbines were deployed, as shown in Table 4. Although efficiency is a critical factor in wind farm design, optimization should first be able to solve a given objective function to obtain the best fitness in the optimization process. Therefore, the results from other studies, including the study by Gray et al., demonstrated the lower park efficiency but improved fitness as more than 39 turbines were deployed. This is because the park efficiency was not included as a parameter in the objective function for the layout optimization. Therefore, the cost model and objective function proposed by Mosetti et al. should be modified in a more reasonable manner. Among previous studies, the results outlined in the study by Parada et al. [19] demonstrated the lowest fitness using 39 turbines, and in turn, Zhang et al. [9] reported the improved results using 40 turbines. However, the fitness of the results of Zhang et al. that were calculated in this study was lower than in the study by Parada et al. Nevertheless, the calculation results of the proposed SA algorithm also indicated that the layout with 40 turbines is optimal, and the regular layout surrounding the wind

farm provides the best fitness result, as shown in Figure 7. This layout is deemed reasonable under the conditions, where the constant wind speed occurs in all directions. Figure 8 shows the fitness variation in case study (b), indicating that it perturbrates to the lower temperature parameter range than case study (a). This is because the solution search area became wider due to an additional wind direction condition that was not considered in case study (a).

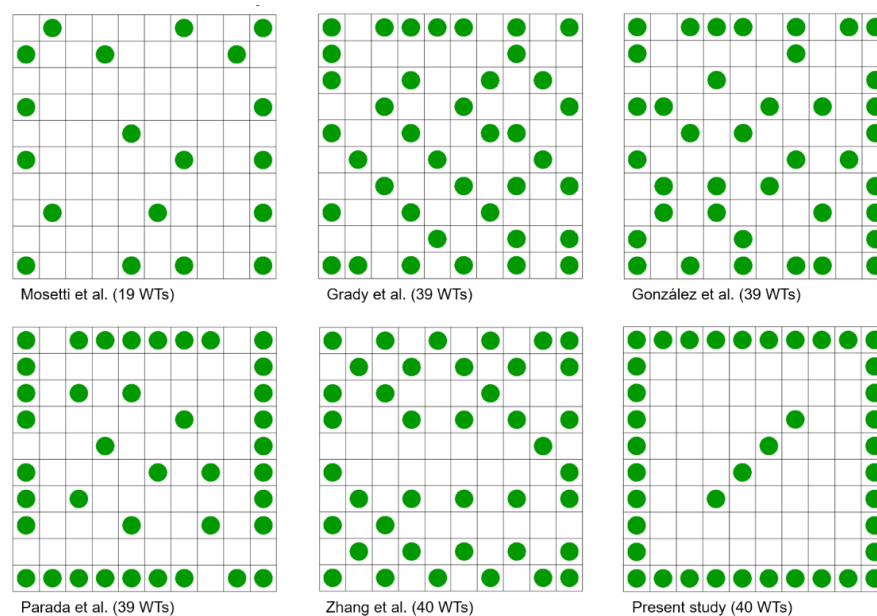


Figure 7. Layout results for case study (b).

Table 4. Layout Results for Case Study (b).

	Number of Turbines	Total Power (kW)	Efficiency (%)	Fitness Value
Mosetti et al. [3]	19	9216 (9244)	93.570 (93.859)	0.0017411 (0.0017371)
Grady et al. [4]	39	17,420 (17,220)	86.165 (85.174)	0.0015454 (0.0015666)
González et al. [8]	39	17,415 (18,065)	86.141 (89.353)	0.0015458 (0.0014903)
Parada et al. [19]	39	17,526 (18,866)	86.688 (93.315)	0.0015361 (0.0014270)
Zhang et al. [9]	40	17,709 (17,991)	85.404 (86.762)	0.0015523 (0.0015280)
Present study	40	18,244	87.983	0.0015068

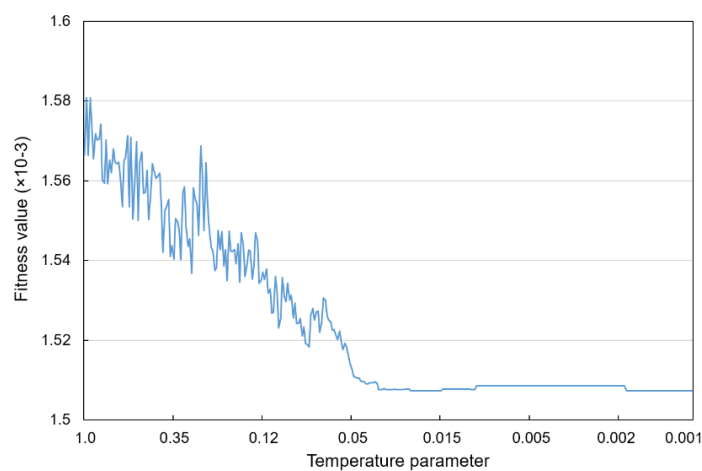


Figure 8. Fitness variation during the process in case study (b).

3.3. Case Study (c): Variable Wind Speed and Multiple Wind Directions

Case study (c) considers 36 wind directions and three wind speeds (8, 12, and 17 m/s) with a different probability of occurrence in each direction. Figure 9 and Table 5 represent the results for case study (c). The study by Mosetti obtained the resulting layout of 15 turbines, which achieved the highest efficiency and worst fitness. Among the considered previous studies, Zhang et al. [9] reported the best fitness results by deploying 40 turbines. In this study, however, the layout of 41 turbines demonstrated the best fitness and improved the results over previous studies. From the layout results obtained in the present study, as shown in Figure 9, it can be seen that the layout pattern does not differ greatly from case study (b). This indicates that similar results were observed as the wind velocity probability at each direction, which was proposed by Mosetti (Figure 4), changed only within the range of 260–350°. Therefore, it can be concluded that the optimal layout condition was derived based on the northwest wind. Moreover, as the change in the wind speed probability is not considered large, it showed a symmetrical pattern. This suggests that even in the study by Zhang et al., which demonstrated good fitness, the symmetrical arrangement is deemed to be the optimal configuration. Figure 10 shows the fitness variation in case study (c), and it can be seen that the SA algorithm demonstrates the best results in case study (c) as well.

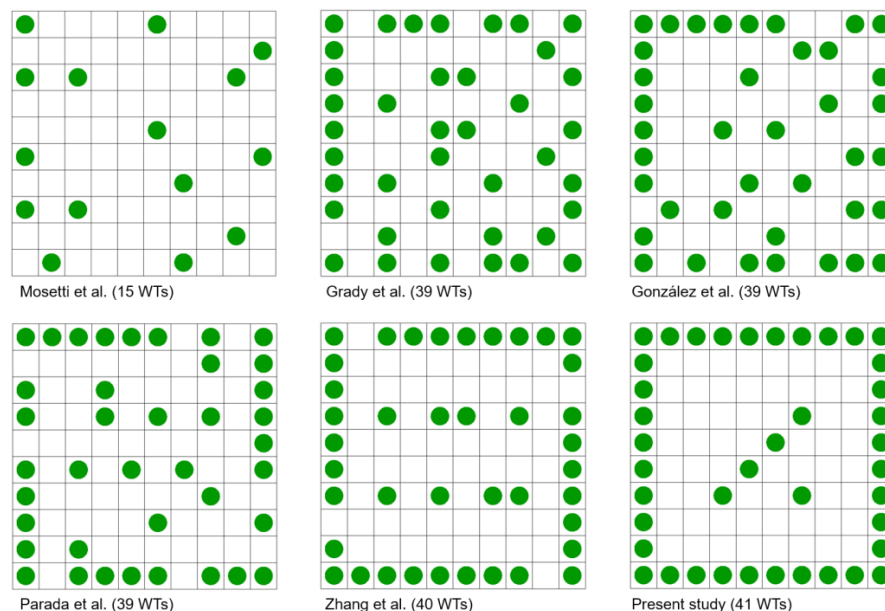


Figure 9. Layout results for case study (c).

Table 5. Layout Results for Case Study (c).

	Number of Turbines	Total Power (kW)	Efficiency (%)	Fitness Value
Mosetti et al. [3]	15	13,319 (13,460)	94.656 (94.620)	0.0010046 (0.0009941)
Grady et al. [4]	39	31,636 (32,038)	86.471 (86.619)	0.0008510 (0.0008403)
González et al. [8]	39	31,984 (32,739)	87.177 (89.487)	0.0008441 (0.0008223)
Parada et al. [19]	39	31,862 (34,173)	87.089 (93.407)	0.0008449 (0.0007878)
Zhang et al. [9]	40	32,868 (34,271)	87.593 (91.333)	0.0008364 (0.0008022)
Present study	41	33,966	88.311	0.0008263

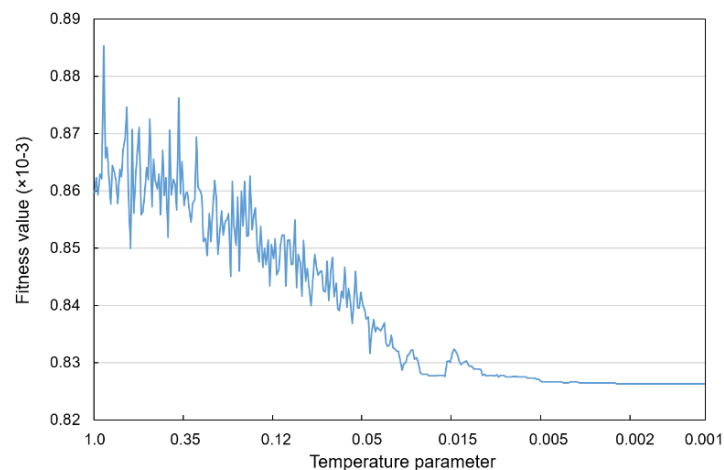


Figure 10. Fitness variation during the process in case study (c).

Figure 11 shows the change in cost per total power and the park efficiency of the wind farm according to the number of wind turbines in case study (c). The cost decreases as the number of wind turbines deployed increases, demonstrating the lowest value at 41 turbines, and then the cost is seen to increase. This shows that 41 is the optimal number of wind turbines for a given cost model at a given wind farm. Contrastingly, park efficiency continues to decline as the number of wind turbines increases. This is because as the turbines are added within a limited area, the wake effects between the turbines subsequently increase. However, the park efficiency is also an important factor, as a simultaneous optimal layout is needed to minimize the costs and maximize park efficiency into the future.

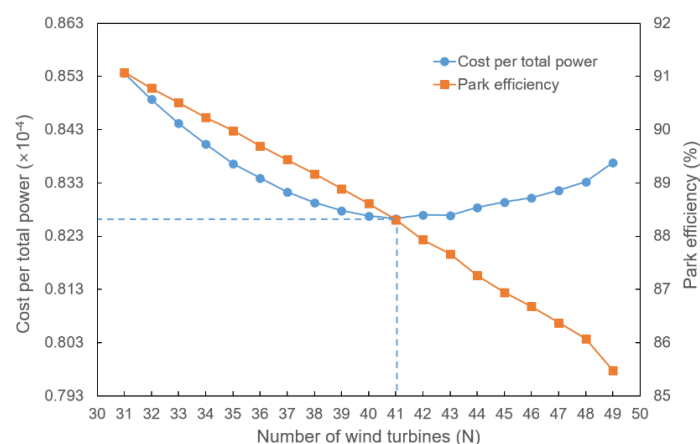


Figure 11. Cost per total power and park efficiency according to the number of wind turbines in case study (c).

4. Conclusions

In this study, an optimization method using the SA algorithm for the wind farm layout optimization problem was proposed and was applied to three scenarios considered in previous studies to evaluate the performance of the optimization algorithm. The performed case studies were as follows: (a) constant wind speed and single wind direction, (b) constant wind speed and multiple wind directions, and (c) variable wind speed and multiple wind directions. The same layout results as in the previous studies were obtained in case study (a) due to the simple wind scenario. In case study (b), a symmetrical layout, which was not observed in previous studies, was obtained and the resulting layout demonstrated the best fitness results. Finally, in case study (c), the SA algorithm demonstrated the optimal number of wind turbines and the layout results that were not observed in previous studies. Most of the compared previous studies use the GA, whereas the SA algorithm in this study demonstrated the best

performance. It should be noted that it is hard to evaluate the performance in terms of the absolute difference. This is due to the fact that optimization algorithms may be applied differently depending on the characteristics of the problem. However, the results indicate that the SA algorithm can be successfully applied to the wind farm layout optimization problem.

In addition, the cost model and the objective function, which were suggested by Mosetti et al. to obtain the optimal layout, have a tradeoff between efficiency and cost, and this problem should be addressed in future works. Finally, to demonstrate the practical applicability of the optimal layout algorithms, more practical wind scenarios need to be examined.

Author Contributions: Conceptualization and methodology, K.Y. and K.C.; software and validation, K.Y.; formal analysis and investigation, K.C.; writing—original draft preparation, K.Y.; writing—review and editing, K.C.

Funding: This work was supported by the research grant of Jeju National University in 2018.

Conflicts of Interest: The authors have no conflict of interest.

References

- Herbert-Acero, J.; Probst, O.; Réthoré, P.-E.; Larsen, G.; Castillo-Villar, K. A Review of Methodological Approaches for the Design and Optimization of Wind Farms. *Energies* **2014**, *7*, 6930–7016. [\[CrossRef\]](#)
- Shakoor, R.; Hassan, M.Y.; Raheem, A.; Wu, Y.K. Wake effect modeling: A review of wind farm layout optimization using Jensen's model. *Renew. Sustain. Energy Rev.* **2016**, *58*, 1048–1059. [\[CrossRef\]](#)
- Mosetti, G.; Poloni, C.; Diviacco, B. Optimization of wind turbine positioning in large windfarms by means of a genetic algorithm. *J. Wind Eng. Ind. Aerodyn.* **1994**, *51*, 105–116. [\[CrossRef\]](#)
- Grady, S.A.; Hussaini, M.Y.; Abdullah, M.M. Placement of wind turbines using genetic algorithms. *Renew. Energy* **2005**, *30*, 259–270. [\[CrossRef\]](#)
- Castro Mora, J.; Calero Barón, J.M.; Riquelme Santos, J.M.; Burgos Payán, M. An evolutive algorithm for wind farm optimal design. *Neurocomputing* **2007**, *70*, 2651–2658. [\[CrossRef\]](#)
- Elkinton, C.N.; Manwell, J.F.; McGowan, J.G. Algorithms for Offshore Wind Farm Layout Optimization. *Wind Eng.* **2008**, *32*, 67–84. [\[CrossRef\]](#)
- Emami, A.; Nogreh, P. New approach on optimization in placement of wind turbines within wind farm by genetic algorithms. *Renew. Energy* **2010**, *35*, 1559–1564. [\[CrossRef\]](#)
- González, J.S.; Gonzalez Rodriguez, A.G.; Mora, J.C.; Santos, J.R.; Payan, M.B. Optimization of wind farm turbines layout using an evolutive algorithm. *Renew. Energy* **2010**, *35*, 1671–1681. [\[CrossRef\]](#)
- Changshui, Z.; Guangdong, H.; Jun, W. A fast algorithm based on the submodular property for optimization of wind turbine positioning. *Renew. Energy* **2011**, *36*, 2951–2958. [\[CrossRef\]](#)
- Chen, Y.; Li, H.; Jin, K.; Song, Q. Wind farm layout optimization using genetic algorithm with different hub height wind turbines. *Energy Convers. Manag.* **2013**, *70*, 56–65. [\[CrossRef\]](#)
- Rahbari, O.; Vafaeipour, M.; Fazelpour, F.; Feidt, M.; Rosen, M.A. Towards realistic designs of wind farm layouts: Application of a novel placement selector approach. *Energy Convers. Manag.* **2014**, *81*, 242–254. [\[CrossRef\]](#)
- Gao, X.; Yang, H.; Lin, L.; Koo, P. Wind turbine layout optimization using multi-population genetic algorithm and a case study in Hong Kong offshore. *J. Wind Eng. Ind. Aerodyn.* **2015**, *139*, 89–99. [\[CrossRef\]](#)
- Mayo, M.; Daoud, M. Informed mutation of wind farm layouts to maximise energy harvest. *Renew. Energy* **2016**, *89*, 437–448. [\[CrossRef\]](#)
- Yamani Douzi Sorkhabi, S.; Romero, D.A.; Yan, G.K.; Gu, M.D.; Moran, J.; Morgenroth, M.; Amon, C.H. The impact of land use constraints in multi-objective energy-noise wind farm layout optimization. *Renew. Energy* **2016**, *85*, 359–370. [\[CrossRef\]](#)
- Wang, L.; Cholette, M.E.; Tan, A.C.C.; Gu, Y. A computationally-efficient layout optimization method for real wind farms considering altitude variations. *Energy* **2017**, *132*, 147–159. [\[CrossRef\]](#)
- Pillai, A.C.; Chick, J.; Khorasanchi, M.; Barbouchi, S.; Johanning, L. Application of an offshore wind farm layout optimization methodology at Middelgrunden wind farm. *Ocean. Eng.* **2017**, *139*, 287–297. [\[CrossRef\]](#)
- Song, M.; Wen, Y.; Duan, B.; Wang, J.; Gong, Q. Micro-siting optimization of a wind farm built in multiple phases. *Energy* **2017**, *137*, 95–103. [\[CrossRef\]](#)

18. Kirchner-Bossi, N.; Porté-Agel, F. Realistic wind farm layout optimization through genetic algorithms using a Gaussian wake model. *Energies* **2018**, *11*, 3268. [[CrossRef](#)]
19. Parada, L.; Herrera, C.; Flores, P.; Parada, V. Wind farm layout optimization using a Gaussian-based wake model. *Renew. Energy* **2017**, *107*, 531–541. [[CrossRef](#)]
20. Kusiak, A.; Song, Z. Design of wind farm layout for maximum wind energy capture. *Renew. Energy* **2010**, *35*, 685–694. [[CrossRef](#)]
21. Kusiak, A.; Zheng, H. Optimization of wind turbine energy and power factor with an evolutionary computation algorithm. *Energy* **2010**, *35*, 1324–1332. [[CrossRef](#)]
22. Song, Z.; Zhang, Z.; Chen, X. The decision model of 3-dimensional wind farm layout design. *Renew. Energy* **2016**, *85*, 248–258. [[CrossRef](#)]
23. Chowdhury, S.; Zhang, J.; Messac, A.; Castillo, L. Unrestricted wind farm layout optimization (UWFLO): Investigating key factors influencing the maximum power generation. *Renew. Energy* **2012**, *38*, 16–30. [[CrossRef](#)]
24. Pookpant, S.; Ongsakul, W. Optimal placement of wind turbines within wind farm using binary particle swarm optimization with time-varying acceleration coefficients. *Renew. Energy* **2013**, *55*, 266–276. [[CrossRef](#)]
25. Hou, P.; Hu, W.; Chen, C.; Soltani, M.; Chen, Z. Optimization of offshore wind farm layout in restricted zones. *Energy* **2016**, *113*, 487–496. [[CrossRef](#)]
26. Ozturk, U.A.; Norman, B.A. Heuristic methods for wind energy conversion system positioning. *Electr. Power Syst. Res.* **2004**, *70*, 179–185. [[CrossRef](#)]
27. Chen, K.; Song, M.X.; Zhang, X.; Wang, S.F. Wind turbine layout optimization with multiple hub height wind turbines using greedy algorithm. *Renew. Energy* **2016**, *96*, 676–686. [[CrossRef](#)]
28. Marmidis, G.; Lazarou, S.; Pyrgioti, E. Optimal placement of wind turbines in a wind park using Monte Carlo simulation. *Renew. Energy* **2008**, *33*, 1455–1460. [[CrossRef](#)]
29. Rivas, R.A.; Clausen, J.; Hansen, K.S.; Jensen, L.E. Solving the Turbine Positioning Problem for Large Offshore Wind Farms by Simulated Annealing. *Wind Eng.* **2009**, *33*, 287–297. [[CrossRef](#)]
30. Eroğlu, Y.; Seçkiner, S.U. Design of wind farm layout using ant colony algorithm. *Renew. Energy* **2012**, *44*, 53–62. [[CrossRef](#)]
31. Kallioras, N.A.; Lagaros, N.D.; Karlaftis, M.G.; Pachy, P. Optimum layout design of onshore wind farms considering stochastic loading. *Adv. Eng. Softw.* **2015**, *88*, 8–20. [[CrossRef](#)]
32. DuPont, B.; Cagan, J.; Moriarty, P. An advanced modeling system for optimization of wind farm layout and wind turbine sizing using a multi-level extended pattern search algorithm. *Energy* **2016**, *106*, 802–814. [[CrossRef](#)]
33. Wagner, M.; Day, J.; Neumann, F. A fast and effective local search algorithm for optimizing the placement of wind turbines. *Renew. Energy* **2013**, *51*, 64–70. [[CrossRef](#)]
34. Archer, R.; Nates, G.; Donovan, S.; Waterer, H. Wind Turbine Interference in a Wind Farm Layout Optimization Mixed Integer Linear Programming Model. *Wind Eng.* **2011**, *35*, 165–175. [[CrossRef](#)]
35. Turner, S.D.O.; Romero, D.A.; Zhang, P.Y.; Amon, C.H.; Chan, T.C.Y. A new mathematical programming approach to optimize wind farm layouts. *Renew. Energy* **2014**, *63*, 674–680. [[CrossRef](#)]
36. Kuo, J.Y.J.; Romero, D.A.; Amon, C.H. A mechanistic semi-empirical wake interaction model for wind farm layout optimization. *Energy* **2015**, *93*, 2157–2165. [[CrossRef](#)]
37. MirHassani, S.A.; Yarahmadi, A. Wind farm layout optimization under uncertainty. *Renew. Energy* **2017**, *107*, 288–297. [[CrossRef](#)]
38. Park, J.; Law, K.H. Layout optimization for maximizing wind farm power production using sequential convex programming. *Appl. Energy* **2015**, *151*, 320–334. [[CrossRef](#)]
39. Guirguis, D.; Romero, D.A.; Amon, C.H. Toward efficient optimization of wind farm layouts: Utilizing exact gradient information. *Appl. Energy* **2016**, *179*, 110–123. [[CrossRef](#)]
40. Tingey, E.B.; Ning, A. Trading off sound pressure level and average power production for wind farm layout optimization. *Renew. Energy* **2017**, *114*, 547–555. [[CrossRef](#)]
41. King, R.N.; Dykes, K.; Graf, P.; Hamlington, P.E. Optimization of wind plant layouts using an adjoint approach. *Wind Energy Sci.* **2017**, *2*, 115–131. [[CrossRef](#)]
42. Du, K.L.; Swamy, M.N.S. Search and optimization by metaheuristics: Techniques and algorithms inspired by nature. In *Search Optimization by Metaheuristics Techniques Algorithms Inspired by Nature*; Birkhäuser: Basel, Switzerland, 2016; pp. 1–434.

43. Jensen, N.O. *A Note on Wind Generator Interaction*; Technical; Risø National Laboratory: Roskilde, Denmark, 1983.
44. Katic, I.; Højstrup, J.; Jensen, N.O. A Simple Model for Cluster Efficiency. In Proceedings of the European Wind Energy Association Conference and Exhibition, Rome, Italy, 7–9 October 1986; pp. 407–410.
45. Brownlee, J. *Clever Algorithms Nature-Inspired Programming Recipes*, 1st ed.; Lulu Press: Morrisville, NC, USA, 2011; ISBN 9781446785065.
46. Yang, K.; Kwak, G.; Cho, K.; Huh, J. Wind farm layout optimization for wake effect uniformity. *Energy* **2019**, *183*, 983–995. [[CrossRef](#)]



© 2019 by the authors. Licensee MDPI, Basel, Switzerland. This article is an open access article distributed under the terms and conditions of the Creative Commons Attribution (CC BY) license (<http://creativecommons.org/licenses/by/4.0/>).